Density functional theory and demixing of binary hard-rod–polymer mixtures

P. Bryk*

Department for the Modeling of Physico-Chemical Processes, Maria Curie-Skłodowska University, 20-031 Lublin, Poland

(Received 26 August 2003; published 24 December 2003)

A density functional theory for a mixture of hard rods and polymers modeled as chains built of hard tangent spheres is proposed by combining the functional due to Yu and Wu for the polymer mixtures [J. Chem. Phys. **117**, 2368 (2002)] with Schmidt's functional [Phys. Rev. E **63**, 50 201 (2001)] for rod-sphere mixtures. As a simple application of the functional, the demixing transition into polymer-rich and rod-rich phases is examined. When the chain length increases, the phase boundary broadens and the critical packing fraction decreases. The shift of the critical point of a demixing transition is most noticeable for short chains.

DOI: 10.1103/PhysRevE.68.062501 PACS number(s): 64.70.Ja, 61.20.Gy, 61.30.Cz

The addition of the nonadsorbing polymer to a monodisperse suspension of colloidal particles can lead to a phase separation due to depletion interactions [1] arising from a tendency of the system to reduce the volume excluded to the polymer coils. One of the simplest theoretical models taking into account this phenomenon is the so-called Asakura-Oosawa (AO) model of colloid-polymer mixtures [2] where the ideal polymer coils (modeled as spheres) can freely interpenetrate each other but the polymer-colloid and colloid-colloid interactions are of the hard sphere type. Initial studies of such systems focused on the bulk phase behavior [3,4], however recently developed density functional theory (DFT) for the AO model [5] initiated investigations of inhomogeneous colloid-polymer mixtures. When brought close to a hard wall, such mixtures may develop a sequence of layering transitions in the partial wetting regime prior to a transition to complete wetting [6,7].

Similar mechanism of fluid-fluid phase separation can be found if other mesoscopic particles such as hard rods are used as depletant agents. Bolhuis and Frenkel (BF) [8] used computer simulations and free volume theory [4] to study bulk phase behavior of mixtures of colloidal hard spheres and vanishingly thin hard rods. They found a surprisingly good agreement (cf Fig. 3 in Ref. [8]) between the free volume theory and Gibbs ensemble Monte Carlo simulations. Although the vanishing thickness and volume constitute a significant simplification (e.g., it rules out the isotropic-nematic transition), the BF model is relevant for some experimental systems, e.g., mixtures of silica spheres and silica coated bohemite rods [9,10]. In order to describe inhomogeneous hard-rod–hard-sphere systems Schmidt [11] proposed a DFT which in its structure closely resembles the AO functional [5]. The functional for the BF model incorporates the exact low-density limit and yields the same equation of state as in Ref. [8]. Moreover, entropic surface phase transitions found previously in model colloid-polymer mixtures close to a hard wall were also recently encountered in hard-rod–hard-sphere mixtures [12]. This further demonstrates deep similarities between the two models.

*Electronic address: pawel@paco.umcs.lublin.pl

The aim of the present work is to construct a functional for a mixture of vanishingly thin hard rods and polymers. Such systems can be regarded as simple microscopic models of the liquid crystal-polymer mixtures. The functional is constructed by combining Schmidt's functional for the BF model with the Yu and Wu [13] functional for mixtures of polymeric fluids. To make this conjecture we take the advantage of the fact that both functionals underlie the fundamental measure theory (FMT) of Rosenfeld [14]. As a simple application we investigate bulk phase diagrams resulting from the proposed theory.

Consider a mixture of hard, vanishingly thin needles (species N) of length L and polymers (species P) modeled as chains composed from M tangentially bonded hard-sphere segments of diameter σ. The hard-sphere monomers building up the chains are freely jointed, i.e., they can adopt any configuration as long as it is free of the intermolecular and intramolecular overlap. The interaction potential between needles $V_{NN}=0$ for all separations, while the pair potential between a polymer segment and a hard rod, V_{PN}, and between two polymer segments, V_{PP}, is of a hard-core type, i.e., is infinite if a pair of objects overlap and zero otherwise. The grand potential of such system as a functional of local densities of polymers $\rho_P(\mathbf{R})$ and needles $\rho_N(\mathbf{r},\boldsymbol{\omega})$ can be written as

$$\begin{aligned}\Omega[\rho_P(\mathbf{R}),\rho_N(\mathbf{r},\boldsymbol{\omega})] &= F_{id}[\rho_P(\mathbf{R}),\rho_N(\mathbf{r},\boldsymbol{\omega})]+F_{ex}[\rho_P(\mathbf{R}),\rho_N(\mathbf{r},\boldsymbol{\omega})] \\ &+ \int d\mathbf{R}\rho_P[(\mathbf{R})(V_{ext}^{(P)}(\mathbf{R})-\mu_P)] \\ &+ \int d\mathbf{r}\int \frac{d\boldsymbol{\omega}}{4\pi}\rho_N(\mathbf{r},\boldsymbol{\omega})[V_{ext}^{(N)}(\mathbf{r},\boldsymbol{\omega})-\mu_N], \end{aligned} \tag{1}$$

where $\mathbf{R}\equiv(\mathbf{r}_1,\mathbf{r}_2,\cdots,\mathbf{r}_M)$ denotes a set of coordinates describing the segment positions, $\boldsymbol{\omega}$ describes the orientation of the rod, $V_{ext}^{(P)}(\mathbf{R})$, μ_P, $V_{ext}^{(N)}(\mathbf{r},\boldsymbol{\omega})$ and μ_N are the external and the chemical potentials for polymers and rods, respectively. The ideal part of the free energy is known exactly

$$\beta F_{id}[\rho_P(\mathbf{R}),\rho_N(\mathbf{r},\boldsymbol{\omega})] = \beta\int d\mathbf{R}\rho_P(\mathbf{R})V_b(\mathbf{R}) + \int d\mathbf{R}\rho_P(\mathbf{R})\{\ln[\Lambda_P^3\rho_P(\mathbf{R})]-1\} + \int d\mathbf{r}\int \frac{d\boldsymbol{\omega}}{4\pi}\rho_N(\mathbf{r},\boldsymbol{\omega})\{\ln[\Lambda_N^3\rho_N(\mathbf{r},\boldsymbol{\omega})]-1\}, \quad (2)$$

where Λ_P and Λ_N are the thermal wavelengths for polymers and needles, respectively. The total bonding potential $V_b(\mathbf{R})$ is a sum of bonding potentials v_b between the segments $V_b(\mathbf{R})=\Sigma_{i=1}^{M-1}v_b(|\mathbf{r}_{i+1}-\mathbf{r}_i|)$ and for the tangential hard spheres this contribution satisfies $\exp[-\beta V_b(\mathbf{R})] = \Pi_{i=1}^{M-1}\delta(|\mathbf{r}_{i+1}-\mathbf{r}_i|-\sigma)/4\pi\sigma^2$.

Within the framework of the fundamental measure theory the excess free energy density Φ is expressed as a simple *function* of the weighted densities $n_\alpha^{(i)}$. We assume that Φ can be represented as a sum of the orientation-independent polymer contribution, Φ_{POL}, and the orientation-dependent polymer-needle contribution, Φ_{PN}. For the orientation-independent contribution we use an extension of Rosenfeld's FMT to the polymeric fluids [13], where the polymer excess free energy density Φ_{POL} is assumed to be a functional of only segment densities $\rho_{PS}(\mathbf{r})$ defined as

$$\rho_{PS}(\mathbf{r}) = \sum_{i=1}^{M}\rho_{PS,i}(\mathbf{r}) = \sum_{i=1}^{M}\int d\mathbf{R}\delta(\mathbf{r}-\mathbf{r}_i)\rho_P(\mathbf{R}), \quad (3)$$

where $\rho_{PS,i}(\mathbf{r})$ is the local density of the segment i of the polymer. Following Ref. [13] we assume that Φ_{POL} can be split into the hard-sphere Φ_{HS} contribution resulting from the hard-sphere repulsion of polymer segments and Φ_P contribution arising due to the chain connectivity. Taking into account the assumptions mentioned above we have $\Phi=\Phi_{PN}+\Phi_{HS}+\Phi_P$. The total excess free energy of the inhomogeneous system is obtained via the integration of the excess free energy density

$$\beta F_{ex} = \int d\mathbf{r}\int\frac{d\boldsymbol{\omega}}{4\pi}\Phi_{PN}(\{n_\alpha^{(i)}\}) + \Phi_{HS}(\{n_\alpha^{(P)}\}) + \Phi_P(\{n_\alpha^{(P)}\}). \quad (4)$$

For the hard-sphere part Φ_{HS} we choose the original Rosenfeld expression [14]

$$\Phi_{HS}(\{n_\alpha^{(P)}\}) = -n_0^{(P)}\ln(1-n_3^{(P)}) + \frac{n_1^{(P)}n_2^{(P)}-\mathbf{n}_{V1}^{(P)}\cdot\mathbf{n}_{V2}^{(P)}}{1-n_3^{(P)}} + \frac{(n_2^{(P)})^3-3n_2^{(P)}\mathbf{n}_{V2}^{(P)}\cdot\mathbf{n}_{V2}^{(P)}}{24\pi(1-n_3^{(P)})^2}. \quad (5)$$

The polymer weighted densities $n_\alpha^{(P)}(\mathbf{r})$ are evaluated via spatial convolutions

$$n_\alpha^{(P)}(\mathbf{r}) = \int d\mathbf{r}'\rho_{PS}(\mathbf{r}')w_\alpha^{(P)}(\mathbf{r}-\mathbf{r}'), \quad (6)$$

where the weight functions $w_\alpha^{(P)}(\mathbf{r})$ are given by

$$w_3^{(P)}(\mathbf{r}) = \Theta\left(\frac{\sigma}{2}-|\mathbf{r}|\right), \quad w_2^{(P)}(\mathbf{r}) = \delta\left(\frac{\sigma}{2}-|\mathbf{r}|\right), \quad (7)$$

$$\mathbf{w}_{V2}^{(P)}(\mathbf{r}) = \frac{\mathbf{r}}{|\mathbf{r}|}\delta\left(\frac{\sigma}{2}-|\mathbf{r}|\right), \quad w_1^{(P)}(\mathbf{r}) = \frac{w_2^{(P)}(\mathbf{r})}{2\pi\sigma}, \quad (8)$$

$$w_0^{(P)}(\mathbf{r}) = \frac{w_2^{(P)}(\mathbf{r})}{\pi\sigma^2}, \quad \mathbf{w}_{V1}^{(P)}(\mathbf{r}) = \frac{\mathbf{w}_{V2}^{(P)}(\mathbf{r})}{2\pi\sigma}. \quad (9)$$

The contribution due to the chain connectivity is evaluated using Wertheim's first-order perturbation theory for a bulk fluid [15] and extended (using FMT-style weighted densities) by Yu and Wu to inhomogeneous systems [13]

$$\Phi_P(\{n_\alpha^{(P)}\}) = \frac{1-M}{M}n_0^P\zeta\ln[y_{hs}(\sigma,\{n_\alpha^{(P)}\})], \quad (10)$$

where $\zeta=1-\mathbf{n}_{V2}^{(P)}\cdot\mathbf{n}_{V2}^{(P)}/(n_2^{(P)})^2$, while y_{hs} is connected with the Carnahan-Starling expression for the contact value of the radial distribution function of a hard-sphere mixture,

$$y_{hs}(\sigma,\{n_\alpha^{(P)}\}) = \frac{1}{1-n_3^{(P)}} + \frac{n_2^{(P)}\sigma\zeta}{4(1-n_3^{(P)})^2} + \frac{(n_2^{(P)})^2\sigma^2\zeta}{72(1-n_3^{(P)})^3}. \quad (11)$$

We note here that both Φ_{HS} and Φ_P are independent on the local density of rods.

To specify the polymer-needle contribution we make use of Schmidt's DFT for hard-rod–hard-sphere mixtures [11] and write the excess free energy density due to vanishingly thin needles as

$$\Phi_{PN}(\{n_\alpha^{(i)}\}) = -n_0^{(N)}\ln(1-n_3^{(P)}) + \frac{n_1^{(N)}n_2^{(PN)}}{1-n_3^{(P)}}. \quad (12)$$

The equation above implies that the polymer-needle contribution to the excess free energy stems solely from the hard-core repulsion between the needle and the hard sphere forming the polymer segment.

The needle weighted densities, $n_\alpha^{(N)}$, are obtained through spatial convolutions of the needle local density and the corresponding orientation-dependent weight functions

$$n_\alpha^{(N)}(\mathbf{r},\boldsymbol{\omega}) = \int d\mathbf{r}'\rho_N(\mathbf{r}',\boldsymbol{\omega})w_\alpha^{(N)}(\mathbf{r}-\mathbf{r}',\boldsymbol{\omega}), \quad \alpha=0,1, \quad (13)$$

while the "mixed" polymer segment-needle weighted density, $n_2^{(PN)}$, is obtained via spatial convolution of the polymer segment density and an orientation-dependent weight function

$$n_2^{(PN)}(\mathbf{r},\boldsymbol{\omega}) = \int d\mathbf{r}'\rho_{PS}(\mathbf{r}')w_2^{(PN)}(\mathbf{r}-\mathbf{r}',\boldsymbol{\omega}). \quad (14)$$

Corresponding weight functions are given as [11]

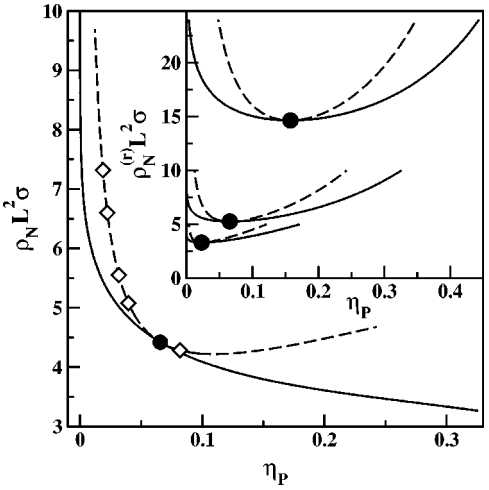

FIG. 1. Phase diagrams for hard-rod–polymer mixtures. Solid and dashed lines denote the binodals and spinodals, respectively. Black circles indicate the critical points of a demixing transition. The main plot shows phase diagram for a mixture of hard rods with size ratio $q=L/\sigma=1$ and hard-sphere 10-mers, in terms of polymer packing fraction $\eta_P=\frac{\pi}{6}\sigma^3 M\rho_P$ and the scaled needle density $\rho_N L^2\sigma$. Open diamonds denote the critical points for a mixture of hard-sphere 10-mers and hard rods with size ratios $q=20$,15,8,5, and 0.1 (from top to bottom). The inset shows the polymer packing fraction-scaled needle reservoir density representation of the phase diagrams for a mixture of hard rods with size ratio $q=1$ and polymers with $M=1$,10, and 100 (from top to bottom).

$$w_1^{(N)}(\mathbf{r},\boldsymbol{\omega})=\frac{1}{4}\int_{-L/2}^{L/2} dl\,\delta(\mathbf{r}+\boldsymbol{\omega}l),$$

$$w_0^{(N)}(\mathbf{r},\boldsymbol{\omega})=\tfrac{1}{2}[\,\delta(\mathbf{r}+\boldsymbol{\omega}l)+\delta(\mathbf{r}-\boldsymbol{\omega}l)\,],$$

$$w_2^{(PN)}(\mathbf{r},\boldsymbol{\omega})=2\left|\boldsymbol{w}_{V2}^{(P)}(\mathbf{r})\cdot\boldsymbol{\omega}\right|. \tag{15}$$

This completes the prescription for the functional. The present theory reduces to Schmidt's functional [11] if $M=1$ and to Yu and Wu functional [13] if the density of rods $\rho_N=0$. Also note that, similar to Ref. [11], the functional is *linear* in the local density of rods.

Although the proposed DFT is intrinsically designed to study inhomogeneous systems, here we restrict ourselves to the isotropic bulk phases where the density of both species are constant. In this case the scalar weighted densities become proportional to the bulk densities of needles and polymers, while the vector weighted densities vanish. Consequently from Eq. (6) we obtain $n_\alpha^{(P)}=\xi_\alpha^{(P)}M\rho_P=\xi_\alpha^{(P)}\rho_{PS}$, with $\xi_3^{(P)}=\pi/6\,\sigma^3$, $\xi_2^{(P)}=\pi\sigma^2$, $\xi_1^{(P)}=\sigma/2$, and $\xi_0^{(P)}=1$. Likewise Eq. (13) yields $n_\alpha^{(N)}=\xi_\alpha^{(N)}\rho_N$, where $\xi_1^{(N)}=L/4$ and $\xi_0^{(N)}=1$. Finally Eq. (14) leads to $n_2^{(PN)}=\xi_2^{(P)}\rho_{PS}$. After inserting the above expressions for the weighted densities into the Eq. (5) and Eqs. (10)–(12) the total free energy per unit volume, Φ_v, is evaluated as $\Phi_v=\Phi_{HS}+\Phi_P+\Phi_{PN}+\beta^{-1}\rho_P[\ln(\rho_P\Lambda_P^3)-1]+\beta^{-1}\rho_N[\ln(\rho_N\Lambda_N^3)-1]$. From Φ_v the pressure p and the chemical potentials of both species are easily calculated

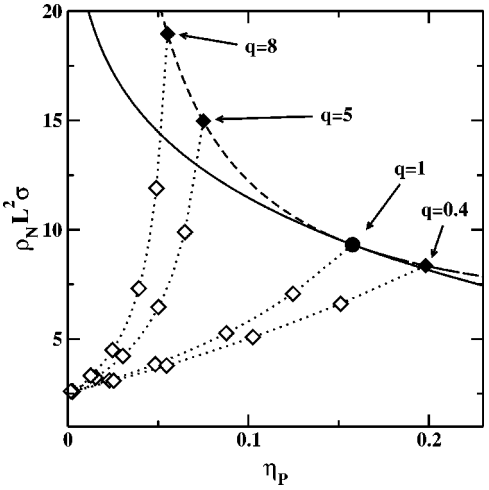

FIG. 2. The phase diagram for a hard-rod–hard-sphere monomer ($M=1$) mixture with the size ratio $q=1$. Solid and dashed lines denote the binodal and the spinodal, respectively. Black diamonds on the spinodal indicate the critical points of a demixing transition for monomer–hard-rod mixtures with different size ratios $q=8$, 5, 1 and 0.4 (from top to bottom). Open diamonds denote the critical points of a demixing transition for a mixture of polymers consisting of M monomers and hard rods for fixed q and for $M=2$, 5, 20, 100, and 10 000 (starting from the right-hand side). Dotted lines serve as a guide to the eye and connect the critical points for the systems with the same size ratio q.

$$\beta p=-\Phi_v+\sum_{j=P,N}\rho_j\frac{\partial\Phi_v}{\partial\rho_j},\quad \beta\mu_j=\frac{\partial\Phi_v}{\partial\rho_j}. \tag{16}$$

Under appropriate conditions a mixture of polymers and hard rods undergoes entropically driven demixing transition to polymer-rich (rod-poor) and polymer-poor (rod-rich) phases. The coexsisting equilibrium densities (binodals) were obtained by solving simultaneously equations for the equality of pressures and chemical potentials in two phases. The spinodals delimiting the regions stable against fluctuations of density and composition were evaluated from the condition $\det[\partial^2\Phi_v/\partial\rho_i\partial\rho_j]=0$, $i,j=P,N$. The critical points were evaluated from

$$s^3\frac{\partial^3\Phi_v}{\partial\rho_P^3}+3s^2\frac{\partial^3\Phi_v}{\partial\rho_P^2\partial\rho_N}+3s\frac{\partial^3\Phi_v}{\partial\rho_P\partial\rho_N^2}+\frac{\partial^3\Phi_v}{\partial\rho_N^3}=0,$$

$$s\equiv\frac{-\partial^2\Phi_v}{\partial\rho_P\partial\rho_N}\Big/\frac{\partial^2\Phi_v}{\partial\rho_P^2}. \tag{17}$$

The above equation arises from the fact that at the critical point the tie-line connecting the coexisting densities becomes tangent to the spinodal line [17].

In Fig. 1 we show examples of binodals (solid lines), spinodals (dashed lines) and critical points (black circles) resulting from the present theory. The phase diagrams plotted in the polymer packing fraction, $\eta_P=\frac{\pi}{6}\sigma^3 M\rho_P$ versus scaled needle reservoir density, $\rho_N^{(r)}L^2\sigma$ representation (see

the inset) were evaluated for systems with $M=1,10,100$ for constant $q=L/\sigma=1$. For the special case $M=1$ (the uppermost diagram) the system reduces to the BF model [16].

As the chain length is increased, the phase boundary becomes more asymmetric and the critical point moves towards lower polymer packing fractions and towards lower reservoir needle densities. Another interesting feature observed in Ref. [11] is that when the polymer packing fraction-*actual* needle density representation instead of the polymer packing fraction-*reservoir* needle density representation is chosen, the critical points for different size ratios q are located on the spinodal of the system with $q=1$. We find the same behavior also in the present model, i.e., for $M>1$. In the main plot of Fig. 1 we show phase diagram for a mixture of 10-mers and hard rods. The critical points for mixtures with different size ratios (open diamonds, from top to bottom for $q=20$, 15, 8, 5, and 0.1) lie on the spinodal for the system with $q=1$ (dashed line).

Let us now consider the limit of very long polymer chains. Intuitively one could argue that in this regime the phase behavior of a needle-polymer mixture should barely depend on the rod length to polymer-segment diameter ratio $q=L/\sigma$ because the physical dimensions of the polymer, e.g., the gyration radius R_g become much bigger than the rod elongation. This scenario is captured within the present theory. In Fig. 2 we show the phase diagram for a mixture of hard-sphere monomers ($M=1$) and hard rods for the size ratio $q=1$. The critical points for different size ratios q (black diamonds) are located on the spinodal. Open diamonds denote the critical points for the systems with $M=2$, 5, 20, 100, and 10 000, respectively. As the chain length increases the critical points for the systems with different size ratios but the same M come closer together and for $M=10\,000$ they virtually merge (on the figure scale) into one point. In the limit $M\to\infty$ the critical scaled needle density tends to the value 2.5526 for all q while the critical polymer packing fraction tends to zero. Similar limiting behavior was found in mixtures of spherical colloids and polymers with excluded volume interactions [18–20].

In conclusion, in this work we propose a DFT for a mixture of vanishingly thin hard rods and polymers modeled as chains built of hard tangent spheres. The functional is constructed by combining the functional due to Yu and Wu for polymer mixtures [13] with Schmidt's functional for hard-rod–hard-sphere mixtures [11]. The proposed theory predicts a demixing transition similar in its nature to that observed for sphere-rod systems. The present functional is well suited to study inhomogeneous systems. It would be of interest to consider a fluid-fluid interface or to investigate surface phase transitions such as entropic wetting or layering that have been discovered in colloid-polymer and colloid-rod mixtures. It is also straightforward to incorporate the Onsager limit [21] of the needle contribution to the functional thus generating a more sophisticated model of inhomogeneous liquid crystal-polymer mixtures. Some of these topics are already under study in our laboratory.

This work has been supported by KBN of Poland under the Grant ''Wpływ samoorganizacji na równowagi fazowe w płynach złożonych.''

[1] S. Asakura and F. Oosawa, J. Chem. Phys. **22**, 1255 (1954).
[2] A. Vrij, Pure Appl. Chem. **48**, 471 (1976).
[3] A.P. Gast, C.K. Hall, and W.B. Russell, J. Colloid Interface Sci. **96**, 251 (1983).
[4] H.N.W. Lekkerkerker, W.C.K. Poon, P.N. Pusey, A. Stroobants, and P.B. Warren, Europhys. Lett. **20**, 559 (1992).
[5] M. Schmidt, H. Löwen, J.M. Brader, and R. Evans, Phys. Rev. Lett. **85**, 1934 (2000).
[6] J.M. Brader, R. Evans, M. Schmidt, and H. Löwen, J. Phys.: Condens. Matter **14**, L1 (2002).
[7] M. Dijkstra and R. van Roij, Phys. Rev. Lett. **89**, 208303 (2002).
[8] P. Bolhuis and D. Frenkel, J. Chem. Phys. **101**, 9869 (1994).
[9] G.A. Vliegenthart and H.N.W. Lekkerkerker, J. Chem. Phys. **111**, 4153 (1999).
[10] G.H. Koenderink, G.A. Vliegenthart, S.G.J.M. Klujitmans, A. van Blaaderen, A.P. Philipse, and H.N.W. Lekkerkerker, Langmuir **15**, 4693 (1999).
[11] M. Schmidt, Phys. Rev. E **63**, 050201 (2001).
[12] R. Roth, J.M. Brader, and M. Schmidt, Europhys. Lett. **63**, 549 (2003).
[13] Y.-X. Yu and J. Wu, J. Chem. Phys. **117**, 2368 (2002).
[14] Y. Rosenfeld, Phys. Rev. Lett. **63**, 980 (1989).
[15] M.S. Wertheim, J. Chem. Phys. **87**, 7323 (1987).
[16] In Ref. [8] the Carnahan-Starling equation of state was used.
[17] J. S. Rowlinson, *Liquids and Liquid Mixtures* (Butterworths, London, 1959), p. 205.
[18] P.G. Bolhuis, A.A. Louis, and J.-P. Hansen, Phys. Rev. Lett. **89**, 128302 (2002).
[19] R.P. Sear, Phys. Rev. E **66**, 051401 (2002).
[20] P. Paricaud, S. Varga, and G. Jackson, J. Chem. Phys. **118**, 8525 (2003).
[21] J.M. Brader, A. Esztermann, and M. Schmidt, Phys. Rev. E **66**, 031401 (2002).